Received: 21 March 2023 | Revised: 31 July 2023 | Accepted: 17 September 2023

DOI: 10.1111/exsy.13463

REVIEW

Expert Systems WILEY

Deep learning methods to detect Alzheimer's disease from MRI: A systematic review

Mariana Coelho [1] | Martin Cerny [2] | João Manuel R. S. Tavares [3]

[1]Faculdade de Engenharia, Universidade do Porto, Porto, Portugal

[2]Faculty of Electrical Engineering and Computer Science of the Technical University of Ostrava, Ostrava, Czech Republic

[3]Instituto de Ciência e Inovação em Engenharia Mecânica e Engenharia Industrial, Departamento de Engenharia Mecânica, Faculdade de Engenharia, Universidade do Porto, Porto, Portugal

Correspondence
João Manuel R. S. Tavares, Instituto de Ciência e Inovação em Engenharia Mecânica e Engenharia Industrial, Departamento de Engenharia Mecânica, Faculdade de Engenharia, Universidade do Porto, Porto, Portugal.
Email: tavares@fe.up.pt

Abstract

Alzheimer's disease (AD) is a progressive and irreversible neurodegenerative condition in the brain that affects memory, thinking, and behaviour. To overcome this problem, which according to the World Health Organization, is on the rise, creating strategies is essential to identify and predict the disease in its early stages before clinical manifestation. In addition to cognitive and mental tests, neuroimaging is promising in this field, especially in assessing brain matter loss. Therefore, computer-aided diagnosis systems have been imposed as fundamental tools to help imaging technicians as the diagnosis becomes less subjective and time-consuming. Thus, machine learning and deep learning (DL) techniques have come into play. In recent years, articles addressing the topic of Alzheimer's diagnosis through DL models are increasingly popular, with an exponential increase from year to year with increasingly higher accuracy values. However, the disease classification remains a challenging and progressing issue, not only in distinguishing between healthy controls and AD patients but mainly in differentiating intermediate stages such as mild cognitive impairment. Therefore, there is a need to develop more valuable and innovative techniques. This article presents an up-to-date systematic review of deep models to detect AD and its intermediate phase by evaluating magnetic resonance images. The DL models chosen by different authors are analysed, as well as their approaches regarding the used dataset and the data pre-processing and analysis techniques.

KEYWORDS
Alzheimer's disease, CAD, deep learning, image analysis, magnetic resonance

1 | INTRODUCTION

One of the most common causes of dementia in the world today is Alzheimer's disease (AD), which can be defined as a progressive and irreversible neurodegenerative disease characterized by abnormal deposition of neurofibrillary tangles and amyloid plaques in the brain, causing issues with memory, thinking, and behaviour (Lee et al., 2019).

According to the World Alzheimer Report (2018), the illness impacted around 50 million individuals in 2018, expected to triple by 2050 (Tanveer et al., 2020). Currently, no treatment can cure a patient who already has AD, but there are drugs and methods to slow down the progression of the disease (Lee et al., 2019).

The brain suffers structural and functional changes because of AD. Alzheimer's disease usually manifests its symptoms beyond the age of 60. Yet, some AD forms develop relatively early (30–50 years) for persons with a genetic mutation. As a result, developing techniques to identify AD before clinical manifestation is critical for timely treatment and slowed progression (Lee et al., 2019).

Patients first have mild cognitive impairment (MCI), progressing to the illness over time. Not all individuals with MCI convert into Alzheimer's patients, though. Therefore, it is necessary to understand the progressive alterations that take place in the brain when AD develops. It is also urgent to find treatments and/or solutions to slow down, stop, reduce the risk of or completely prevent the onset of this disease (Tanveer et al., 2020).

In recent years, several computer-aided diagnosis (CAD) systems have been created to aid in disease diagnosis and follow-up. Between 1970 and 1990, the first rule-based models were created, and subsequently, supervised models were designed. To create these supervised models, it was necessary to extract pertinent features from the input data, which required the intervention of human experts, which is a tedious and very time-consuming task. Nevertheless, with the emergence of deep learning (DL) models, drawing out the used features directly from the data without recourse to human interaction became possible. Therefore, researchers have focused on creating DL models to accurately diagnose several diseases, including AD (Sethi et al., 2022).

Mainly as to AD, neuroimaging has proved to be extremely important in identifying early changes in brain tissue that may be related to the disease. A wide range of brain imaging measurements continues to be developed for the scientific research and clinical evaluation of Alzheimer's disease. Structural magnetic resonance imaging (sMRI) is one of the best-established procedures for early identification and monitoring of AD, as can be seen in Figure 1 (Reiman & Jagust, 2012).

This review is focused on investigating DL-based CAD systems for Alzheimer's disease detection in MRI, which has been a growing research and technological sector in recent years, as can be realized from Figure 2. Accordingly, the DL models that different authors have proposed are analysed, as well as the used database(s), the applied pre-processing steps, and the chosen methodology to handle the input data and its computational classification.

Several literature reviews targeting the same problem have been published recently, such as Goyal et al. (2022), Sharma et al. (2023), and Shukla et al. (2023). However, the current review is up-to-date and aims at the following contributions:

1. Introduces DL algorithms to detect AD from magnetic resonance (MR) images;
2. Discusses datasets that have been used to diagnose AD;
3. Analyses current state-of-the-art approaches for classifying AD in MR images;
4. Compares existing DL algorithms as to their efficiency.

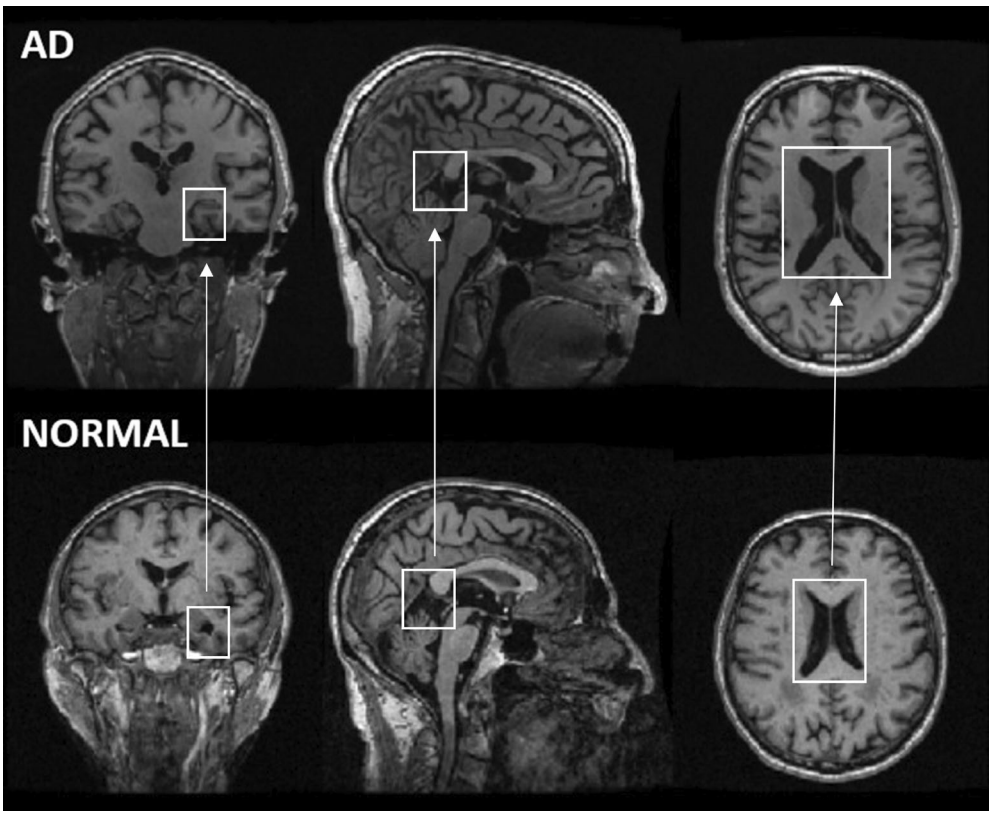

FIGURE 1 Examples of MRI images of the brain of an Alzheimer's patient and a healthy person taken from the Alzheimer's disease neuroimaging initiative (ADNI) database (ADNI (n.d.). These images have morphological differences, which are identified in each of the images, between normal controls and Alzheimer's patients that can be perceived by magnetic resonance imaging.

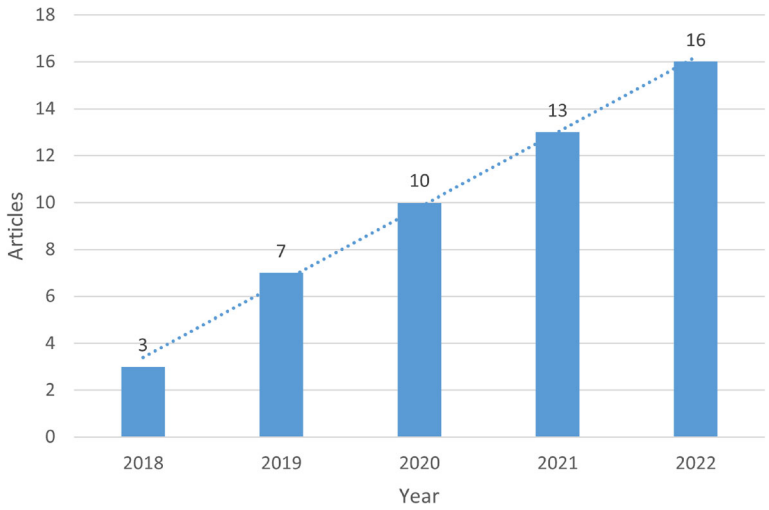

FIGURE 2 Articles gathered from the Scopus database published within the previous 5 years, according to Section 3.

This article is organized according to the following structure: Section 2 includes a contextualization of the existing DL techniques; the methodology used for articles gathering and selection is described in Section 3; then, Section 4 is divided into four subsections, according to the topics usually involved in the development of a project of this type, namely: used dataset(s), data pre-processing, data analysis, DL models, data augmentation, and transfer learning; finally, Section 5 presents a discussion and conclusions in Section 6.

2 | DEEP LEARNING

DL is a topic of great interest in many scientific fields, particularly in medical image analysis. Currently, DL is the most effective machine-learning method in many medical applications. The concept of 'deep learning' refers to using a deep neural network, which accepts multiple signals as input, linearly combines them using weights, and then these combined values undergo non-linear processes to produce the final result (Razzak et al., 2018). A DL network generally has two characteristics: several layers of nonlinear processing units and supervised or unsupervised learning of feature presentations on each layer. The first DL framework was developed on top of an artificial neural network in the 1980s, yet it was not until 2006 that neural networks started to have a meaningful influence (Cao et al., 2018). Researchers use various types of DL models such as convolutional neural network (CNN), deep neural network (DNN), recurrent neural network (RNN), deep conventional extreme learning machines (DCELM), deep Boltzmann machine (DBM), deep belief network (DBN), deep autoencoder (dA), and their variants. A summary (Cao et al., 2018; Razzak et al., 2018) of the current DL models for AD diagnosis as to their main characteristics and advantages and disadvantages is given in Table 1.

3 | ARTICLES SELECTION METHODOLOGY

In the Scopus database, a systematic literature search was performed, Figure 3, using the following query: 'ALL ('Alzheimer's Disease') AND ('image' OR 'imaging') AND ('MR' OR 'Magnetic Resonance') AND ('T1') AND ('Deep Learning') AND ('MCI' OR 'mild cognitive impairment') AND ('3D' OR '3 dimensional') AND ('classification') AND (TITLE ('Alzheimer')) AND (LIMIT-TO (DOCTYPE, 'ar')) AND (LIMIT-TO (PUBYEAR, 2023) OR LIMIT-TO (PUBYEAR, 2022) OR LIMIT-TO (PUBYEAR, 2021) OR LIMIT-TO (PUBYEAR, 2020) OR LIMIT-TO (PUBYEAR, 2019) OR LIMIT-TO (PUBYEAR, 2018)) AND (LIMIT-TO (LANGUAGE, 'English'))'. A search using the same criteria was performed in the PUBMED database, but no additional articles were found.

In the performed search, a total of 94 articles were obtained; of these, 51 were found useful for the topic under review. The remaining were excluded for the following reasons: the proposed method does not classify the input data, does not include DL techniques, or does not use 3D MR T1 images.

TABLE 1 Different deep learning models that have been used to detect AD (adapted from Razzak et al. (2018)).

DL model	Details	Pros	Cons	Reference
Convolutional neural network (CNN)	Three-layer network: a convolutional, a pooling, and a fully connected layer. It is very interesting for two-dimensional (2D) data since it applies convolutional filters that transform 2D data into three-dimensional (3D) data. There are different types of CNN architectures, including AlexNet, LeNet, faster region-based convolutional neural network (R-CNN), GoogleNEt, residual network (ResNet), visual geometry group network (VGGNet), and ZFnet.	Excellent performance, quick learning.	A significant amount of labelled data is necessary.	Basheera and Ram (2020)
Deep neural network (DNN)	Network with three or more layers, implementing complex non-linear connections. It can be applied either for classification or regression.	It is commonly employed and quite accurate.	The training procedure is challenging since the error is passed down to the previous individual layers, and they get much smaller. The model's learning rate is likewise far too sluggish.	Raghavaiah and Varadarajan (2021)
Recurrent neural network (RNN)	RNN uses sequential data or time series data. As sequential data is used, the weights are shared at all stages. They differ from other methods because they employ data from earlier inputs to alter current input and output. There are many variations, including long short-term memory (LSTM), bidirectional long short-term memory (BLSTM), multi-dimensional long short-term memory (MDLSTM), and hierarchical long short-term memory (HLSTM).	It can model time dependencies.	Numerous problems arise due to a vanishing gradient and the demand for large datasets.	Cui and Liu (2019b)
Deep conventional extreme learning machine (DCELM)	Convolutional neural networks' ability to abstract features and extreme learning machines' quick training speed are combined in DCELM. This network employs a Gaussian probability function for local connection sampling.	It is quite accurate and commonly utilized. It is a quick and efficient training technique in terms of computing. For random distortion, it works well.	Initialization might be successful if the learning function is fairly straightforward and there is minimal labelled data.	-
Deep Boltzmann machine (DBM)	The Boltzmann family of machines is the basis for this model. It constructs the probability distribution using an energy function, then refines the parameters until the model understands the true distribution of the data. It is made up of one-way links among all hidden layers.	As top-down feedback is applied, there is ambiguous data for more robust interference.	With large datasets, parameter optimization is not feasible.	-
Deep belief network (DBN)	DBN uses one-way connections and is applied to both supervised and unsupervised learning. Each sub-network's hidden layers act as the following layer's visible layer.	The likelihood is maximized directly by the greedy approach employed in each layer and the tractable inference.	The training method requires a lot of processing power, given the initialization.	-
Deep autoencoder (dA)	Is inserted in unsupervised learning and was developed mainly to extract and/or reduce the dimensionality of the features. The quantity of inputs is equal to the quantity of outputs. There are numerous variants: de-noising autoencoder, sparse autoencoder, and conventional auto-encoder for increased robustness.	It does not need labelled data.	It requires a step before training. Its training may not converge.	Mendoza-Léon et al. (2020)

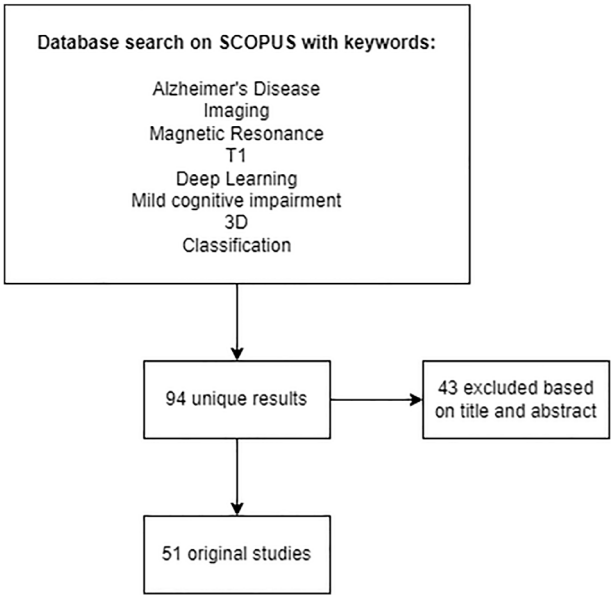

FIGURE 3 PRISMA diagram showing the performed literature search in the Scopus database.

4 | REVIEW RESULTS

4.1 | Used datasets

The data used in any machine learning algorithm is fundamental to the final solution. The quantity of data and its quality, in terms of annotations and the way it is organized, must be evaluated with special attention before applying any model to it. This section presents a description of the datasets used in the reviewed articles.

4.1.1 | Alzheimer's disease neuroimaging initiative

The purpose of the Alzheimer's disease neuroimaging initiative (ADNI) study is to analyse the brain's structure and function across the course of different disease states using biomarkers and clinical measurements to track the progression of the disease. The project was created in 2004 and consists of four studies: ADNI1, ADNIGO, ADNI2, and ADNI3, in each of which new participants are being added while the original participants continue to be monitored. This dataset also has a wide variety of data types, namely: clinical information as to demographics, physical examinations, and cognitive assessment data, genetic information, MR images, including structural MRI, functional MRI (fMRI), and diffusion tensor imaging (DTI) images, positron emission tomography (PET) images, including amyloid PET, fluorodeoxyglucose (FDG) PET, and Tau PET, and biospecimens, that is, blood, urine, and cerebrospinal fluid (CSF), images (ADNI, n.d.).

4.1.2 | Open Access Imaging Studies series

The Open Access Imaging Studies series (OASIS) project makes brain neuroimaging datasets available to help researchers develop this field. Four studies have already been developed in this initiative: OASIS-1, OASIS-2, OASIS-3, and OASIS-4, and being a neuroimaging database, three imaging modalities are available: MRI, PET, and computed tomography (CT) (OASIS, n.d.).

4.1.3 | Australian Imaging, Biomarker and Lifestyle Flagship Study of Ageing

The Australian Imaging, Biomarker and Lifestyle Flagship Study of Ageing (AIBL) is a study whose major aim is to investigate which biomarkers, mental characteristics, and health and lifestyle aspects are determinants in the development of Alzheimer's disease. This dataset includes neuroimaging data such as MRI and PET data, lifestyle data, that is, questionnaires on diet, sleeping habits and so forth cognitive testing, family history, and biomarkers: blood samples and CSF (AIBL, n.d.).

TABLE 2 Main characteristics of the datasets mostly referenced in the reviewed articles.

Dataset	No. of patients	Type of images	Availability	URL	Articles
ADNI	1821	MRI; PET	Public	https://adni.loni.usc.edu/	Agarwal et al. (2022), Asl et al. (2018), Angkoso et al. (2022), Bae et al. (2020, 2021), Basaia et al. (2019), Basheera and Ram (2020), Bi et al. (2021), Cobbinah et al. (2022), Cui and Liu (2019a, 2019b), Dyrba et al. (2021), Faisal and Kwon (2022), Fan et al. (2021), Folego et al. (2020), Goenka and Tiwari (2022), Guan et al. (2022), Hazarika et al. (2021), Huang et al. (2019), Jiang et al. (2022), Khagi et al. (2021), Li and Liu (2018, 2019), Li, Wei, et al. (2022), Liu et al. (2019), Liang et al. (2022), Lim et al. (2022), Liu et al. (2020, 2022), Mendoza-Léon et al. (2020), Nanni et al. (2020), Ocasio and Duong (2021), Qasim Abbas et al. (2023), Raghavaiah and Varadarajan (2021, 2022), Razzak et al. (2022), Sampath and Baskar (2022), Shaji et al. (2021), Suh et al. (2020), Wang et al. (2022), Wen et al. (2020), Yan et al. (2022), Zhang et al. (2019), Zhao et al. (2021)
OASIS	3059	MRI; PET; CT	Public	https://aibl.csiro.au/	Folego et al. (2020), Sampath and Baskar (2022), Saratxaga et al. (2021), Suh et al. (2020), Wen et al. (2020), Yiğit and Işik (2020), Zhao et al. (2021)
AIBL	1000+	MRI; PET	Public	https://www.oasis-brains.org/	Dyrba et al. (2021), Fan et al. (2021), Folego et al. (2020), Sampath and Baskar (2022), Wen et al. (2020)

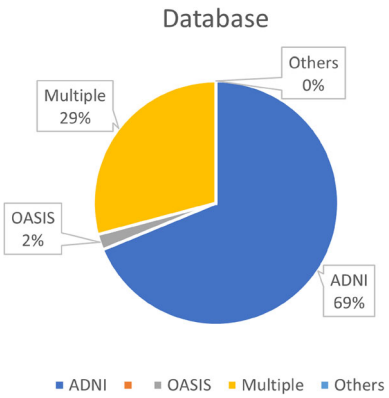

FIGURE 4 Prevalence of the used datasets in the reviewed articles.

Table 2 presents complementary information of these datasets, which are mostly referenced in the reviewed articles and have the greatest variety of information. Still, it is a common practice to use several datasets, as can be perceived from Figure 4. The datasets and related articles are identified in Table 3.

4.2 | Data pre-processing

After acquiring the neuroimages, using the respective imaging modality, to be analyzed, it is necessary to understand how these will be inputted into the DL architecture employed for diagnosing AD. However, before this process, the used images are usually submitted to several data pre-processing steps. Particularly, the pre-processing aims to enhance the input data by ensuring that all the images have a degree of parity that, in turn, makes the following steps, for example, as to image segmentation and feature extraction, more effective. It entails removing artifacts, changing image resolution, and correcting contrast disparities caused by differing imaging acquisition hardware and parameters (Vadmal et al., 2020).

4.2.1 | Bias field correction

The bias field, often known as intensity inhomogeneity, is a low-frequency spatially changing of MRI artifacts that results in smooth fluctuations in signal intensity within tissues with similar physical qualities. The magnetic field strength is directly proportional to the bias field. The produced

TABLE 3 Summary of the approaches found in this review.

Reference	Year	Dataset(s)	Image type(s)	Subjects	Data pre-processing	Data processing	Feature extraction	Classifier(s)	Accuracy metric(s)
Li, Wei, et al. (2022)	2022	ADNI	T1 sMRI	928 subjects: 330 CN, 299 MCI, 299 AD	Resample skull stripping intensity correction register clip	Whole 3D image		U-Net	AD vs. CN: 93.16% MCI vs. CN: 80.44%
Sampath and Baskar (2022)	2022	ADNI AIBL OASIS	T1 sMRI	6400 subjects: 3200 CN, 2240 SMC, 896MCI, 64 AD	Resizing adaptive filtering for noise removal adaptive histogram equalization	Whole 3D image	GLCM Gabor filter wavelet features HSICL	FSODSNN based classifier	ADNI. CN vs. SMC vs. MCI vs. AD: 99.89% AIBL. CN vs. SMC vs. MCI vs. AD: 99.67% OASIS. CN vs. SMC vs. MCI vs. AD: 99.61%
Raghavaiah and Varadarajan (2022)	2022	ADNI		955 subjects: 273 CN, 432 MCI, 250 AD	Skull-stripping normalization TC-BWO-FCM for CSF, WM and GM segmentation	ROI-based	TECD features + Clinical features	HRF-DNN	AD vs. CN: 98.68% MCI vs. AD: 95.88% MCI vs. CN: 97.23%
Raghavaiah and Varadarajan (2021)	2021	ADNI		280 subjects: 89 CN, 122 MCI, 69 AD	Bias field correction normalization CSF, WM and GM segmentation spatial smoothing	ROI-based	Gabor filter	Optimal DNN	AD vs. CN: 96.43% MCI vs. AD: 94.64% MCI vs. CN: 91.07%
Wang et al. (2022)	2022	ADNI J-ADNI	T1 sMRI Non-image information: cognitive scores, Age and APOE type	800 subjects: 200 CN, 200 EMCI, 400 MCI, 200 AD	Image shape normalization Image intensity normalization skull-stripping hippocampi (L/R) and anterior temporal lobes (L/R) segmentation data augmentation	ROI-based	DenseNet-121 + AE + SA	Linear SVM	87.80%
Li and Liu (2019)	2019	ADNI	T1 sMRI	807 subjects: 216 CN, 233 sMCI, 164 pMCI, 194 AD	Intensity homogenization affine registration skull-stripping hippocampus segmentation data augmentation	ROI-based + Patch-based		3D DenseNet for Feature learning + Bidirectional gated recurrent unit (BGRU)	AD vs. CN: 89.10% MCI vs. CN: 75.00% pMCI vs. sMCI: 72.50%
Liu et al. (2020)	2020	ADNI	T1 sMRI	449 subjects: 119 CN, 233 MCI, 97 AD	Skull-stripping N3 bias field correction Affine registration Hippocampus Segmentation Data augmentation	ROI-based + Patch-based		1. Multi-task deep CNN 2. 3D DenseNet 3. Multi-task deep CNN + 3D DenseNet	1. AD vs. CN: 80.10% MCI vs. CN: 71.50% 2. AD vs. CN: 86.60% MCI vs. CN: 74.10% 3. AD vs. CN: 88.90% MCI vs. CN: 76.20%
Basheera and Ram (2020)	2020	ADNI	T1 sMRI T2 sMRI - results not presented	120 subjects: 20 CN, 25 MCI, 70 AD	Skull stripping data augmentation	Slice-based		CNN	AD vs. CN: 55.00% MCI vs. AD: 51.00% MCI vs. CN: 19.00% AD vs. MCI vs. CN: 34.00%
Guan et al. (2022)	2021	ADNI	T1 sMRI	1340 subjects: 394 CN, 401 sMCI, 197 pMCI, 348 AD	Reorientation cropping bias field correction normalization skull-stripping data augmentation	Whole 3D image		pABN	AD vs. NC: 90.70% pMCI vs. sMCI: 79.30%
Folego et al. (2020)	2020	ADNI AIBL CADD MIRIAD OASIS	T1 sMRI		Intensity winsorizing bias field correction translation alignment rigid transformation affine	Whole 3D image		LeNet-5 VGG 512 GoogLeNet ResNet	VGG 512 + CADDementia. CN vs. MCI vs. AD: 52.30%

(Continues)

TABLE 3 (Continued)

Reference	Year	Dataset(s)	Image type(s)	Subjects	Data pre-processing	Data processing	Feature extraction	Classifier(s)	Accuracy metric(s)
					transformation skull-stripping normalization				
Li and Liu (2018)	2018	ADNI	T1 sMRI	831 subjects: 229 CN, 403 MCI, 199 AD	Intensity homogenization Skull-stripping Linear registration	Patch-based		DenseNet	AD vs. CN: 89.50% MCI vs. CN: 73.80%
Liang et al. (2022)	2022	ADNI	T1 sMRI	8751 subjects: 832 CN, 419 AD		Whole 3D image		DMRNet	AD vs. CN: 89.30%
Asl et al. (2018)	2018	ADNI	T1 sMRI	210 subjects: 70 CN, 70 MCI, 70 AD	Spatially normalization Skull-stripping Normalization	Whole 3D image	3D-CAE	3D-DSA-CNN	AD vs. CN: 99.31% AD vs. MCI: 100.00% MCI vs. CN: 94.20% AD + MCI vs. CN: 95.73% AD vs. MCI vs. CN: 94.80%
Goenka and Tiwari (2022)	2022	ADNI	T1 sMRI	769 subjects: 475 CN, 224 MCI, 70 AD	N4 bias field correction skull stripping rigid registration	1. Whole 3D image 2. Patched-based 3. Slice-based		ConvNet	1. AD vs. CN: 97.83% AD vs. MCI: 98.68% CN vs. MCI: 99.10% CN vs. MCI vs. AD: 98.26% 2. AD vs. CN: 98.37% AD vs. MCI: 98.14% CN vs. MCI: 97.72% CN vs. MCI vs. AD: 97.48% 3. AD vs. CN: 97.39% AD vs. MCI: 96.25% CN vs. MCI: 94.31% CN vs. MCI vs. AD: 95.37%
Li, Wang, et al. (2022)	2022	ADNI	T1 sMRI	503 subjects: 116 CN, 187 MCI, 200 AD	Standardized voxel values Size scaling Skull Stripping Image registration	Slice-Based		1. CCS-ResNet-18 2. CCS-ResNet-50	1. AD vs. CN: 94.34% AD vs. MCI: 95.72% CN vs. MCI: 89.44% CN vs. MCI vs. AD: 88.31% 2. AD vs. CN: 97.90% AD vs. MCI: 96.23% CN vs. MCI: 91.75% CN vs. MCI vs. AD: 88.61%
Hazarika et al. (2021)	2021	ADNI	T1 sMRI	210 subjects 70 CN, 70 MCI, 70 AD	Size scaling skull stripping	Slice-based		LeNet	AD vs. CN: 95.00% AD vs. MCI: 97.00% MCI vs. CN: 97.00%
Odusami et al. (2022)	2022	ADNI		138 subjects: 25 CN, 25 SMC, 25 EMCI, 13 MCI, 25 LMCI, 25 AD	Resizing cropping formalization	Slice-Based	ResNet18 DenseNet121	Randomized concatenated deep features-based classification system	(Weight Initialization-Kaiming) AD vs. CN vs. MCI: 98.21% AD vs. MCI vs. LMCI vs. CN: 93.06% MCI vs. LMCI vs. EMCI vs. AD vs. CN: 98.86%
Yiğit and Işik (2020)	2020	OASIS MIRIAD	T1 sMRI	485 subjects: 339 CN, 116 MCI, 30 AD	Skull stripping Data augmentation Size scaling CLAHE Smoothing	Slice-Based		CNN	AD vs. MCI: 82.00%
Bi et al. (2021)	2021	ADNI		578 subjects: 188 CN, 210 MCI, 180 AD	CSF, WM and GM segmentation skull stripping			1. CNN 2. DML	1. AD vs. CN: 81.00% MCI vs. CN: 63.00% 2. AD vs. CN: 83.00% MCI vs. CN: 65.00%
Basaia et al. (2019)	2018	ADNI Milan	T1 sMRI	1638 subjects: 407 CN, 813 MCI, 418 AD	Registration CSF, WM and GM segmentation normalization data augmentation	Whole 3D image		CNN	AD vs. CN: 98.20% cMCI vs. CN: 87.70% sMCI vs. CN: 76.40% AD vs. cMCI: 75.80% AD vs. sMCI: 86.30% cMCI vs. sMCI: 74.90%

TABLE 3 (Continued)

Reference	Year	Dataset(s)	Image type(s)	Subjects	Data pre-processing	Data processing	Feature extraction	Classifier(s)	Accuracy metric(s)
Faisal and Kwon (2022)	2019	ADNI	T1 sMRI	489 subjects: 163 CN, 163 MCI, 163 AD	Size scaling	Slice-based		CNN	AD vs. MCI vs. CN: 96.12 %
Shaji et al. (2021)	2021	ADNI	T1 sMRI	200 subjects: 100 CN, 100 AD	Spatial normalization skull-stripping data augmentation	Slice-based		Inception-ResNet	AD vs. MCI:69.00%
Nanni et al. (2020)	2020	ADNI	T1 sMRI	773 subjects: 162 CN, 234 ncMCI, 240 cMCI, 137 AD	Reorientation cropping skull-stripping co-registration GM segmentation	Slice-based whole 3D image		1. AlexNet 2. GoogleNet 3. ResNet50 4. ResNet101 5. InceptionV3 6. CNN	1. AD vs. CN: 90.80% cMCI vs. CN: 84.20% cMCI vs. ncMCI: 69.10% 2. AD vs. CN: 89.60% cMCI vs. CN: 81.60% cMCI vs. ncMCI: 70.00% 3. AD vs. CN: 89.80% cMCI vs. CN: 81.80% cMCI vs. ncMCI: 70.40% 4. AD vs. CN: 89.90% cMCI vs. CN: 82.20% cMCI vs. ncMCI: 71.20% 5. AD vs. CN: 88.80% cMCI vs. CN: 79.90% cMCI vs. ncMCI: 69.80% 6. AD vs. CN: 84.10% cMCI vs. CN: 72.30% cMCI vs. ncMCI: 61.10%
Wen et al. (2020)	2020	ADNI AIBL OASIS	T1 sMRI	1951 subjects: 835 CN, 311 sMCI, 315 pMCI, 490 AD	Bias field correction intensity rescaling linear registration or non-linear registration and skull-stripping	1. 3D subject-based 2. 3D ROI-based 3. 3D patch-based 4. 2D slice-based		CNN	1. AD vs. CN: 77. 33% (baseline) sMCI vs. pMCI: 60.50% (baseline) AD vs. CN: 79.66% (longitudinal) sMCI vs. pMCI: 61.50% (longitudinal) 2. AD vs. CN: 80.66% (baseline) sMCI vs. pMCI: 67.00% (baseline) AD vs. CN: 79.66% (longitudinal) sMCI vs. pMCI: 65.50% (longitudinal) 3. AD vs. CN: 75.33% (baseline) sMCI vs. pMCI: 67.00% (baseline) AD vs. CN: 79.00% (longitudinal) sMCI vs. pMCI: 57.00% (longitudinal) 4. AD vs. CN: 72.33% (baseline) AD vs. CN: 69.33% (longitudinal)
Lim et al. (2022)	2022	ADNI	T1 sMRI	819 subjects: 229 CN, 398 MCI, 192 AD	Skull-stripping non-uniform intensity correction CSF, WM and GM segmentation pixel values normalization data augmentation	Slice-based + ROI-based		1. CNN 2. VGG-16 3. ResNet-50	1. AD vs. CN vs. MCI:72.70% 2. AD vs. CN vs. MCI: 78.57% 3. AD vs. CN vs. MCI: 75.71%
Ocasio and Duong (2021)	2021	ADNI	T1 sMRI	557 subjects: 320 CN, 237 AD	Non-uniform intensity normalization (N3) correction skull-stripping linear registration intensity normalization data augmentation	Whole 3D image		1. Single time point CNN 2. Dual time point CNN (12 months)	1. AD vs. CN: 86.00% sMCI vs. pMCI: 2. AD vs. CN: 88.70% sMCI vs. pMCI

(Continues)

TABLE 3 (Continued)

Reference	Year	Dataset(s)	Image type(s)	Subjects	Data pre-processing	Data processing	Feature extraction	Classifier(s)	Accuracy metric(s)
Suh et al. (2020)	2020	ADNI OASIS private databases	T1 sMRI	2727 subjects: 1432 CN, 743 MCI, 552 AD		Whole 3D image	deep CNN	XGBoost	AD vs. MCI: 79.53% MCI vs. CN: 74.76% AD vs. CN: 91.17%
Liu et al. (2022)	2022	ADNI		520 subjects: 160 CN, 200 MCI, 160 AD	Slice timing head movement correction size scaling WM and GM S	Slice-based + ROI-based		MSC-Net	GM. AD vs. CN: 97.91% AD vs. MCI: 94.44% MCI vs. CN: 90.74% WM. AD vs. CN: 98.96% AD vs. MCI: 95.37% MCI vs. CN: 92.60%
Huang et al. (2019)	2019	ADNI	T1 sMRI FDG-PET	1211 subjects: 731 CN, 441 sMCI, 326 pMCI, 647 AD	Reorientation resample	Whole 3D image		VGG	MRI. CN vs. AD: 81.19% multi-modal. CN vs. AD: 90.10% CN vs. pMCI: 82.38% sMCI vs. pMCI: 72.22%
Agarwal et al. (2022)	2022	ADNI	T1 sMRI	719 subjects: 245 CN, 229 sMCI, 245 AD	N4 bias correction denoising brain extraction affine registration	Whole 3D image		1. DenseNet 2. EfficientNet	1. AD vs. CN: 99.55% sMCI vs. AD: 82.06% 2. AD vs. CN: 91.55% sMCI vs. AD: 81.38%
Cui and Liu (2019a)	2019	ADNI	T1 sMRI	811 subjects: 223 CN, 231 sMCI, 165 pMCI, 192 AD	Non-uniform intensity normalization (N3) correction skull-stripping rigid registration hippocampus segmentation data augmentation	ROI-based + Patch-based		DenseNet	AD vs. CN: 90.12% pMCI vs. sMCI: 73.23% MCI vs. CN: 73.02%
Bae et al. (2020)	2020	ADNI SNUBH	T1 sMRI	780 subjects: 390 CN, 390 AD	Skull-stripping rigid transformation	Slice-based		Inception V4	AD vs. CN:92.50%
Dyrba et al. (2021)	2021	ADNI AIBL DELCODE	T1 sMRI Amyloid AV45-PET	663 subjects (254 CN, 220 MCI, 189 AD) - ADNI-GO/2 575 subjects (326 CN, 187 MCI, 62 AD) - ADNI-3 606 subjects (448 CN, 96 MCI, 62 AD) - AIBL 474 subjects (215 CN, 155 MCI, 104 AD) - DELCODE	WM and GM segmentation spatial normalization data augmentation	ROI-based		CNN	ADNI-GO/2. MCI vs. CN: 74.50% AD vs. CN: 88.90% ADNI-3. MCI vs. CN: 63.10% AD vs. CN: 84.40% AIBL. MCI vs. CN: 68.20% AD vs. CN: 85.00% DELCODE. MCI vs. CN: 71.00% AD vs. CN: 85.50%
Saratxaga et al. (2021)	2021	OASIS	T1 sMRI	741 subjects: 513 CN, 168 very-mild dementia, 55 mild dementia, 5 moderate dementia)	Normalization data augmentation	1. Slice-based 2. Whole 3D image 3. Slice-based		1. BrainNet2D 2. BrainNet3D 3. ResNet18	1. CN vs. others: 86.50% 2. CN vs. others: 82.00% 3. CN vs. others: 87.00%
Zhang et al. (2019)	2019	ADNI private database	T1 sMRI 18F-FDG PET	392 subjects: 101 CN, 200 MCI, 91 AD		Slice-based		VGGNet-19	MRI. AD vs. CN: 95.12% CN vs. MCI: 83.24% AD vs. MCI: 82.41% multi-modal. AD vs. CN: 95.89% CN vs. MCI: 85.74% AD vs. MCI: 88.20%

TABLE 3 (Continued)

Reference	Year	Dataset(s)	Image type(s)	Subjects	Data pre-processing	Data processing	Feature extraction	Classifier(s)	Accuracy metric(s)
Angkoso et al. (2022)	2021	ADNI	T1 sMRI	449 subjects: 500 CN, 500 MCI, 500 AD	Skull-stripping spatially normalization linear registration	Slice-based		Mp-CNN	CN vs. MCI vc AD: 93.00%
Razzak et al. (2022)	2022	ADNI	T1 sMRI	379 subjects: 146 CN, 138 MCI, 95 AD	Resizing cropping data augmentation	ROI-based		1. DenseNet 2. PartialNet	1. AD vs. CN vs. MCI: 96.72% AD vs. CN: 80.11% AD vs. MCI: 96.65% MCI vs. CN: 97.76% 2. AD vs. CN vs. MCI: 98.23% AD vs. CN: 87.11% AD vs. MCI: 99.26% MCI vs. CN: 100.00%
Zhao et al. (2021)	2021	ADNI OASIS	T1 sMRI		CSF, WM and GM segmentation linear registration cropping	ROI-based + Patch-based		mi-GAN	
Yan et al. (2022)	2022	ADNI	T1 sMRI	139 subjects: 55 CN, 84 AD	Template registration skull-stripping filter denoising intensity normalization	Patch-based	SE mechanism PSA mechanism +FCN	MLP	AD vs. CN: 98.85%
Cobbinah et al. (2022)	2022	ADNI	T1 sMRI T2 sMRI	1125 subjects: 375 CN, 375 MCI, 375 AD	Data augmentation	Whole 3D image	CAAE	CRAT	AD vs. CN: 91.90% AD vs. MCI: 90.05% MCI vs. CN: 88.10%
Cui and Liu (2019b)	2019	ADNI	T1 sMRI	830 subjects: 229 CN, 236 sMCI, 167 pMCI, 198 AD	Anterior commissure (AC) - posterior commissure (PC) correction skull-stripping nonuniform intensity normalization (N3) CSF, WM, and GM segmentation data augmentation	ROI-based		1. CNN 2. RNN 3. CNN + RNN	1. AD vs. CN: 88.99% pMCI vs. sMCI: 70.22% 2. AD vs. CN: 85.01% pMCI vs. sMCI: 68.49% 3. AD vs. CN: 91.33% pMCI vs. sMCI: 71.71%
Mendoza-Léon et al. (2020)	2020	OASIS	T1 sMRI	174 subjects: 87 CN, 87 AD	Field-bias intensity correction spatial image normalization skull-stripping	Slice-based + Patch-based		SSA	Axial. CN vs. AD: 87.50% Coronal. CN vs. AD: 90.00% Sagittal. CN vs. AD: 90.00%
Bae et al. (2021)	2020	ADNI	T1 sMRI	3940 subjects: 2084 CN, 222 ncMCI, 228 cMCI, 1406 AD	Skull stripping reorientation cropping padding correct intensity inhomogeneity (N3)	Whole 3D image		ResNet29	ncMCI vs. cMCI: 82.40%
Qasim Abbas et al. (2023)	2022	ADNI	T1 sMRI	238 subjects: 154 CN, 84 AD	ACPC alignment correction intensity correction for uniform homogeneity skull-stripping registration	Whole 3D image	JD	CNN	AD vs. CN: 96.61%
Fan et al. (2021)	2021	ADNI AIBL	T1 sMRI	204 subjects: 65 CN, 56 EMC, 40 LMCI, 43 AD	Skull-stripping sampling clipping intensity normalization	Whole 3D image		U-net	AD vs. CN: 95.71% CN vs. EMCI: 87.98% EMCI vs. LMCI: 90.14% LMCI vs. AD: 90.05% CN vs. EMCI vs. LMCI vs. AD: 86:47%
Jiang et al. (2022)	2022	ADNI	T1 sMRI Amyloid PET non-image information:	417 subjects: 236 CN, 181 preAD	CSF, WM and GM segmentation normalization smoothing	Slice-based + ROI-based	AlexNet ZFNet ResNet18 ResNet34	SVM	AlexNet. CN vs. preAD: 87.91% ZFNet. CN vs. preAD: 87.91% ResNet18. CN vs. preAD: 87.67% ResNet34. CN vs.

(Continues)

TABLE 3 (Continued)

Reference	Year	Dataset(s)	Image type(s)	Subjects	Data pre-processing	Data processing	Feature extraction	Classifier(s)	Accuracy metric(s)
			cognitive scores, Age and APOE type				InceptionV3 Xception		preAD: 89.53% InceptionV3. CN vs. preAD: 84.88% Xception. CN vs. preAD: 88.84%
Liu et al. (2019)	2019	ADNI BIOCARD	T1 sMRI	3304 subjects (at scan time - 1417 CN, 1146 MCI, 741 AD) 3304 subjects (latest diagnosis - 1266 CN, 926 MCI, 1112 AD)	Skull-stripping reorientation intensity normalization inhomogeneity correction	Whole 3D image	LDDMM MALF	Siamese Net	At scan time.CN vs. (MCI + AD): 91.03% latest diagnosis. CN vs. (MCI + AD): 92.20%
Khagi et al. (2021)	2021	ADNI GARD	T1 sMRI	188 subjects (74 CN, 40 MCI, 74 AD) - ADNI 123 subjects (42 CN, 39 MCI, 42 AD) - GARD	Normalization registration CSF, WM and GM segmentation smoothing	ROI-based		BR-FNN	ADNI (ROI_CL). AD vs. CN: 88.67% AD vs. MCI: 72.86% ADNI (ROI_AAL). AD vs. CN: 78.22% AD vs. MCI: 80.57% GARD (ROI_CL). AD vs. CN: 71.67% AD vs. MCI: 59.75% GARD (ROI_AAL). AD vs. CN: 75.60% AD vs. MCI: 42.35%
Basher et al. (2021)	2021	GARD	T1 sMRI	252 subjects: 171 CN, 81 AD	Normalization data augmentation	Patch-based + Slice-based + ROI-based	DVE-CNN	DNN	L Hippocampus (LH). AD vs. CN: 76.26% right hippocampus (RH). AD vs. CN: 77.34%

Abbreviations: aAD, asymptotic Alzheimer's disease; cMCI, mild cognitive impaired converting to AD; CN, cognitively normal; EMCI, early mild cognitive impairment; LMCI, late mild cognitive impairment; MCI, mild cognitive impairment; MID, mild demented; MOD, moderate demented; ncMCI, mild cognitive impaired not converting to AD; ND, non-demented; pMCI, progressive MCI; preAD, individuals at risk of Alzheimer's disease (according to standard uptake ratio > 1.18 calculated by amyloid PET) SMC, significant memory concern; sMCI, stable MCI; VMD, very mild demented.

bias field is almost invisible when images are acquired at 0.5T and can be discarded. However, the bias field is powerful enough to cause issues and significantly impact the MRI analysis when images are scanned with a field of 1.5T, 3T, or greater (Despotović et al., 2015). So, the bias filed correction is a technique that has been usually used in this field (Agarwal et al., 2022; Basheera & Ram, 2020; Cui & Liu, 2019a, 2019b; Folego et al., 2020; Goenka & Tiwari, 2022; Guan et al., 2022; Jiang et al., 2022; Li & Liu, 2018, 2019; Liu et al., 2019; Mendoza-Léon et al., 2020; Ocasio & Duong, 2021; Qasim Abbas et al., 2023; Raghavaiah & Varadarajan, 2021; Wang et al., 2022; Wen et al., 2020).

4.2.2 | Normalization

Another method of pre-processing that has been commonly used in this field is normalization (Asl et al., 2018; Basaia et al., 2019; Basher et al., 2021; Fan et al., 2021; Folego et al., 2020; Guan et al., 2022; Jiang et al., 2022; Khagi et al., 2021; Liu et al., 2019; Ocasio & Duong, 2021; Raghavaiah & Varadarajan, 2021, 2022; Saratxaga et al., 2021; Wang et al., 2022; Yan et al., 2022), which aims to reduce the grey (or colour) values in an image to a single set of relative grey (or colour) values. This guarantees that differences in imaging acquisition parameters across different imaging scanners do not strongly affect the further results since similar tissues show up in a consistent range of values throughout all image scans (Vadmal et al., 2020).

4.2.3 | Skull stripping

Skull stripping, also called brain extraction, is a computational approach for removing non-essential tissues from a brain image, such as skull, fat, or skin. In this way, the amount of non-interesting information can be reduced, and the subsequent feature extraction step can be easier (Vadmal et al., 2020). This method is one of the most widely used in this field (Agarwal et al., 2022; Angkoso et al., 2022; Asl et al., 2018; Bae et al., 2020; Basheera & Ram, 2020; Bi et al., 2021; Cui & Liu, 2019a, 2019b; Fan et al., 2021; Folego et al., 2020; Goenka & Tiwari, 2022; Guan et al., 2022; Hazarika et al., 2021; Li & Liu, 2018, 2019; Li, Wang, et al., 2022; Li, Wei, et al., 2022; Lim et al., 2022; Liu et al., 2019, 2020; Mendoza-Léon et al., 2020; Nanni et al., 2020; Ocasio & Duong, 2021; Qasim Abbas et al., 2023; Raghavaiah & Varadarajan, 2022; Shaji et al., 2021; Wang et al., 2022; Yan et al., 2022; Yiğit & Işik, 2020).

4.2.4 | Spatial smoothing

This technique increases the signal-to-noise ratio by removing the high-frequency spatial noise components and is applied in several imaging modalities, including MRI. Averaging data pixels (or voxels in 3D) with their neighbours is called spatial smoothing. Sharp 'edges' of the images are blurred as a result, and spatial correlation within the data becomes more prominent (Mansour et al., 2022). It should be noted that, although this technique is commonly used in medical image processing, in the field under study, it has not shown a great advantage, and, therefore, it is only referred to in one of the reviewed articles.

4.2.5 | Registration

Image registration is characterized by a process of overlaying two or more images containing the same object of study but taken at various times, from different perspectives, and/or by different imaging modalities. This step has been commonly used in this field (Agarwal et al., 2022; Angkoso et al., 2022; Asl et al., 2018; Bae et al., 2020, 2021; Basaia et al., 2019; Cui & Liu, 2019a; Dyrba et al., 2021; Folego et al., 2020; Goenka & Tiwari, 2022; Li & Liu, 2018, 2019; Li, Wang, et al., 2022; Li, Wei, et al., 2022; Liu et al., 2020; Ocasio & Duong, 2021; Razzak et al., 2022; Shaji et al., 2021; Zhao et al., 2021), and implies discovering the transformation between the images to be registered so that their main characteristics are spatially aligned. Mainly, this alignment can be rigid or affine. A rigid transformation is composed of six parameters with translation and rotation and is usually used in intrasubject registration when the object of attention is not relatively deformed, for example, for images at the same stage of brain development. The affine transformation is often used if scaling and skewing are involved, such as in the case of different subjects or different developmental brain stages (Despotović et al., 2015).

4.3 | Data analysis

From the pre-processed brain images, to classify subjects into different categories, such as AD or cognitively normal (CN), it is usually necessary to extract and analyse features from the pre-processed images. Thus, this process commonly includes several steps like feature extraction, selection, and classification. Yet, for most researchers, the challenge is to know how to tackle and input the neuroimages into the classifier, and for

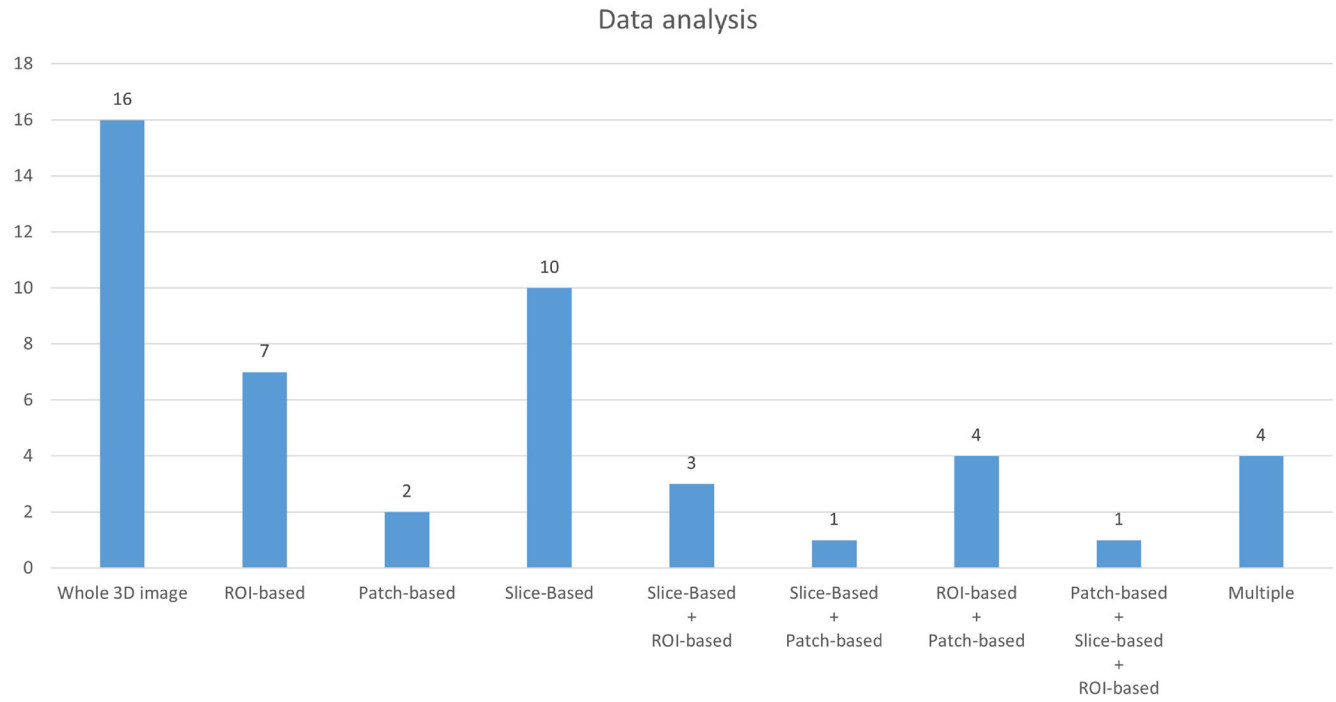

FIGURE 5 Prevalence of the used data processing approaches in the reviewed articles: Number of works where the techniques are used individually (whole 3D image, ROI-based, patch-based, and slice-based), of works where they are used in combination (slice-based + ROI-based, slice-based + patch-based, ROI-based + patch-based, and patch-based + slice-based + ROI-based), and of works that tested more than one approach individually (multiple).

that, different data processing approaches can be used, such as whole image, slice, region of interest (ROI), and patch-based, as described in the following sections and summarized in Figure 5.

- Whole 3D image

This kind of approach uses as input the whole 3D image, which allows preserving all the spatial information of the original image as well as all the details in the image, and has been commonly adopted by most researchers (Agarwal et al., 2022; Asl et al., 2018; Bae et al., 2021; Basaia et al., 2019; Cobbinah et al., 2022; Fan et al., 2021; Folego et al., 2020; Guan et al., 2022; Huang et al., 2019; Li, Wei, et al., 2022; Liang et al., 2022; Liu et al., 2019; Ocasio & Duong, 2021; Qasim Abbas et al., 2023; Sampath & Baskar, 2022; Suh et al., 2020), however, it entails high computational costs.

- Slice-based

The slice-based approach extracts 2D images from the original 3D image to obtain data features. This enables the removal of background areas that act as interference; however, part of the information in the original 3D image is lost. The authors in Hazarika et al. (2021), Li, Wang, et al. (2022), Suh et al. (2020) selected slices in the coronal plane that contained the hippocampus region, as it is very relevant in diagnosing AD. In Yiğit and Işik (2020), the same strategy was used; however, instead of one plane, the original 3D image is sliced according to three planes: coronal, axial, and sagittal planes.

To not lose so much relevant information, the author in Faisal and Kwon (2022) only removes the first and last slices, as they usually do not contain any useful detail.

Two completely different approaches were adopted by Shaji et al. (2021) and Angkoso et al. (2022). The first authors, of the 182 slices of each image, only used the mid-axial slice in their study, while the second authors, for each plane, used the slice with the largest area and the ones immediately before (-1) and after ($+1$) it.

- ROI-based

The approach based on regions of interest involves segmenting particular anatomical structures from the original images, such as white matter (WM), grey matter (GM), cerebrospinal fluid, and/or hippocampus. This technique allows focusing the DL model on the most relevant areas

linked to the disease; however, other relevant structures cannot be considered in the model. Multiple authors have used this technique (Cui & Liu, 2019b; Dyrba et al., 2021; Khagi et al., 2021; Raghavaiah & Varadarajan, 2021; Raghavaiah & Varadarajan, 2022; Razzak et al., 2022; Wang et al., 2022).

- Patch-based

As the designation implies, the patch-based approach splits the original image into small patches that are used as input to extract features. Like the two previous approaches, this one also allows reducing the amount of performed calculations required by the used DL classifier; however, there is a loss of spatial information between the patches. The authors of Li and Liu (2018), Yan et al. (2022) applied this technique in their study.

- Combination

It is also possible to use more than one of the previous approaches simultaneously, for example, ROI-based + Patch-based, Slice-based + ROI-based, or Slice-based + Patch-based. As to the first option, three works (Cui & Liu, 2019a; Li & Liu, 2019; Liu et al., 2020; Zhao et al., 2021) used it and extracted patches centred in the ROI of the hippocampus. On the other hand, as in the second case, basically, the regions of interest are extracted from 2D images instead of the original 3D image. Examples of this approach can be found in Huang et al. (2019), Lim et al. (2022), and Mendoza-Léon et al. (2020). The latter option was found in article (Mendoza-Léon et al., 2020), which divided the slices into multiple patches. In addition, article (Basher et al., 2021) tested the combination of the Patch-, Slice-, and ROI-based approaches.

4.4 | Deep learning based approaches

The construction of the AD classification pipeline, namely the selection of the type of neural network to be implemented, the definition of its hyperparameters, and the method for its validation and evaluation, are the usual last steps in the development of computational systems to diagnose AD, and the researchers have adopted many different approaches. Nevertheless, two major paths can be taken in this process: either classify directly or perform a feature extraction process before the classification step. Both paths were found in the performed review. In addition to classification approaches, prediction approaches were also found in a much smaller number.

4.4.1 | Classification approaches

Most researchers directly applied a classifier to the original or pre-processed images. In the field of image analysis, CNNs have attracted most of the attention due to being specially designed to recognize patterns. Basheera and Ram (2020), Faisal and Kwon (2022) and Yiğit and Işik (2020) applied 2D CNNs, while Basaia et al. (2019) and Dyrba et al. (2021) opted for a 3D CNN. An interesting study was taken by Wen et al. (2020), who used a CNN to compare the influence of different data processing approaches. The authors conclude that the results show the superiority of 3D approaches over 2D approaches, but there was little difference in the outcomes of the different 3D approaches. In addition to CNNs, their variants have also been applied in this field, namely U-net (Fan et al., 2021; Li, Wei, et al., 2022), DenseNet (Agarwal et al., 2022; Cui & Liu, 2019a; Li & Liu, 2018; Liu et al., 2020; Razzak et al., 2022), ConvNet (Goenka & Tiwari, 2022), ResNet (Bae et al., 2021; Folego et al., 2020; Li, Wang, et al., 2022; Lim et al., 2022; Nanni et al., 2020; Saratxaga et al., 2021; Shaji et al., 2021), LeNet (Folego et al., 2020; Hazarika et al., 2021), AlexNet (Nanni et al., 2020), GoogleNet (Folego et al., 2020; Nanni et al., 2020), Inception (Bae et al., 2020; Nanni et al., 2020; Shaji et al., 2021), EfficientNet (Agarwal et al., 2022), VGG (Folego et al., 2020; Huang et al., 2019; Ocasio & Duong, 2021; Zhang et al., 2019), and MSCNet (Liu et al., 2022).

Accordingly, Liu et al. (2022) applied an MSCNet to segment WM and GM in images and proved that WM is more effective in AD diagnosing. On the other hand, Goenka and Tiwari (2022) applied a ConvNet to different types of data processing approaches, concluding that the whole 3D image approach, in contrast to the patch and slice-based approaches, led to the maximum accuracy. Folego et al. (2020) compared multiple DL architectures, namely LeNet-5, VGG 512, GoogLeNet, and ResNet, and obtained better results using the VGG 512 architecture. Another type of approach was adopted by some authors who, instead of implementing only one DL network, used a combination of two or more networks to obtain better results. An example of this is the case of Cui and Liu (2019b) who combined a CNN with an RNN: the first model is used to extract the spatial features of each time point and obtain a single time classification result; then, the RNN model, which is based on a cascaded bidirectional gated recurrent unit (BGRU), is used to tackle the temporal fluctuations and produce the longitudinal features used to enhance the final classification. Liu et al. (2020) also chose to combine two CNNs, using a multi-task deep CNN model to capture the multi-level features for hippocampal joint segmentation and disease classification, while the 3D deep DenseNet model picks up the characteristics from hippocampal image

patches for the disease classification. Both the multi-task and the DenseNet models were trained individually, and the final classification was carried out by a fully connected layer followed by a softmax layer that was carefully calibrated. In Li and Liu (2019), Li et al. used a very similar reasoning: constructed hybrid convolutional and recurrent neural networks based on DenseNets and BGRU networks for the inner and outer hippo patches separately. 3D DenseNets were built on the patches to learn more specific image and shape features of the hippocampus for classification, while stacked BGRUs were utilized to record the high-level correlation and asymmetry features between the right and left hippocampus. In the end, two fully connected layers were attached to merge the features that the hybrid neural networks had learned from the inner and outer patches of the hippocampus to improve the final classification.

Additionally to the common use of CNNs and RNNs, Mendoza-Léon et al. (2020) developed supervised switching autoencoders (SSAs) to conduct AD classification using just a sMRI slice.

4.4.2 | Feature extraction + classification approaches

The other path taken by the reviewed articles consisted in applying a network that extracted features from the images and then applying a classifier that allowed obtaining a diagnosis for AD.

In this sense, several researchers have chosen to use DL models to extract the features that are then linked to simpler machine learning algorithms to perform the final classification. For example, Wang et al. (2022) implemented a DenseNet with self-attention (SA) and auto-encoding (AE) to obtain the features that served as input to a linear support vector machine (SVM) classifier that performed the classification. Suh et al. (2020) employed a deep CNN model, which divides each brain image into 82 areas. The used approach combines a target section with nearby slices in the channel dimension and feeds this information into the XGBoost module that classifies the patients. Finally, Jiang et al. (2022) implemented a deep learning radiomics (DLR) model to extract features from MR images that are then combined with clinical information and classified using an SVM. Several architectures were tested for the DRL model: AlexNet, ZFNet, ResNet18, ResNet34, InceptionV3, and ResNet34 proved to be the best.

DNN also proved to be a widely used model as a classifier followed by a feature extractor. Raghavaiah and Varadarajan (2021) applied a Gabor filter, Raghavaiah and Varadarajan (2022) developed a hybrid texture, edge, colour, and density (TECD) feature extraction approach paired with clinical data, and Basher et al. (2021) built a discrete volume estimator CNN model to identify positions of the left and right hippocampus.

Two groups of authors chose to use a deep Siamese neural network (DSNN): Liu et al. (2019) mapped several atlases using a large diphomorphic deformation metric mapping (LDDMM) and then got the atlas plot labels for each imaging scan through the multi-atlas likelihood fusion (MALF) algorithm before applying the neural network; while Sampath and Baskar (2022) utilized grey-level co-occurrence matrices (GLCM), Gabor, and wavelet features to extract the MR image's biomarker data and a Hilbert Schmidt independence criteria lasso (HSICL) algorithm to select the most preponderant features.

Cobbinah et al. (2022) implemented a convolutional adversity autoencoder (CAAE) to lessen the existing variations in multi-centre raw scans by storing them in an aligned common space. Subsequently, a convolutional residual soft attention network (CRAT) was also intended for AD classification. While in Asl et al. (2018), a 3D convolutional autoencoder (3D-CAE) was developed to extract features followed by the application of a 3D deeply supervised adaptive CNN (3D-DSA-CNN) to perform task-specific classification.

In Yan et al. (2022), chose to implement attention mechanisms to enhance the performance of CNNs significantly. Thus, the authors added squeeze and excitation (SE) and pyramid squeeze attention (PSA) mechanisms to the fully convolutional network (FCN) model to obtain the information from each image regarding the disease probability map. In addition, they also built a multi-layer perceptron (MLP) classifier, combining a disease probability map's feature information with the age, gender, and mini-mental state examination (MMSE) of each sample to obtain the final classification. Finally, Odusami et al. (2022) suggested concatenating deep and random weight features taken from the ResNet18 and DenseNet121 networks, which simultaneously learned DL features from MR images.

4.4.3 | Time-to-event prognostic approaches

In addition to the classification from MR images at the different AD phases, some works are focused on predicting the evolution of the disease. In this regard, Zhao et al. (2021) proposed a new paradigm for predicting disease progression that embraces five cases of evolution: MCI-AD, MCI-MCI, MCI-CN, CN-MCI, and CN-CN. In the process, a patch-based 3D mi-GAN model was developed to produce high-quality images at future time points with two innovations: implementing a 3D U-Net based network conditioning on image patches and additional knowledge, that is, age, academic level, gender, and APOE, in BL; modifying the final objective function by adding a gradient difference loss (GDL loss) and a mean square error loss in image space and frequency domain. The 3D U-Net based model can utilize the multi-scale characteristics of input image patches and the additional data. The generator can create less blurry and more reliable images due to the GDL loss. Then, the created whole-brain 3D images are fed into a trained 3D ternary classification model to identify their phases and better track the development of the disease within four years.

In Ocasio and Duong (2021), a prediction model was developed with two alternatives. A single time point CNN that, for classification, a single 3D MRI with a full-time point of patients diagnosed with AD or CN served as the input and had as the output the CN versus AD binary classification, and for prediction, a single 3D MRI with a full-time point of patients diagnosed with MCI was served as the input, and the outcome was a forecast of whether the patient had advanced (pMCI) or stayed stable (sMCI) 3 years later. A second approach was a dual time point CNN, where the input consisted of 3D MRI scans taken at both baseline and 12 months later, utilizing the same study group, and output classes used at a single time point for classification and prediction. Both types of models started with a sequence of convolutional blocks, flattened into at least one fully connected layer, concluding with a decision of classification or prediction.

4.5 | Data augmentation and transfer learning

Big data is widely used by deep neural networks to prevent overfitting. Regrettably, common neuroimaging datasets of AD patients are not so big. To overcome this problem, two strategies can be applied to imaging datasets with small samples: data augmentation and transfer learning (Al-Qerem et al., 2021).

Data augmentation is an effective strategy to enhance the performance of learning algorithms by increasing the samples. This strategy is characterized by performing transformations on already existing images, such as rotation, flipping, and cropping (Al-Qerem et al., 2021). About 32% of the reviewed studies implement this strategies, namely Basaia et al. (2019), Basheera and Ram (2020), Basher et al. (2021), Cobbinah et al. (2022), Cui and Liu (2019a, 2019b), Dyrba et al. (2021), Guan et al. (2022), Li and Liu (2019), Lim et al. (2022), Liu et al. (2020), Ocasio and Duong (2021), Razzak et al. (2022), Saratxaga et al. (2021), Shaji et al. (2021), Wang et al. (2022), and Yiğit and Işik (2020). As an example, this strategy was implemented by Dyrba et al. (2021) who, by applying flipping along the coronal (R/L) axis and also a translation of $+/-$ 10 voxels in each direction (x/y/z) to all original images, obtaining about fourteen times more samples.

Transfer learning is an ML technique where a model already created for one task is used as a baseline for another task. In other words, this technique proposes storing information learned from solving one problem and using it to solve another related challenge (Al-Qerem et al., 2021). Multiple studies have opted for this procedure, namely, the ones in Bae et al. (2021), Basher et al. (2021), Faisal and Kwon (2022), Folego et al. (2020), Guan et al. (2022), Hazarika et al. (2021), Li and Liu (2018), Lim et al. (2022), Nanni et al. (2020), Ocasio and Duong (2021), Saratxaga et al. (2021), and Wen et al. (2020). A study demonstrating this method's importance was developed by Nanni et al. (2020), who investigated the effect of the transfer learning technique on several DL models. Briefly, the study assessed the efficacy of transfer learning techniques on DL models trained on common images and then applied to sMR images of the brain. The models used were AlexNet, GoogleNet, ResNet50, ResNet101, and InceptionV3. As opposed to a 3D CNN model trained from scratch on MRI volumes, the results showed a performance increase of at least 4.7% in terms of accuracy.

5 | DISCUSSION

Aiming to classify/distinguish between the various Alzheimer's disease phases using MR imaging modality, 49 different approaches were found, which are summarized in Table 3.

It is very difficult to define which methods are best, given the different nuances that it is possible to create across the computational pipeline as described in Section 3. However, different evaluation metrics were used in the reviewed articles, such as accuracy (Acc), sensitivity, F1 score, specificity, precision, recall, and under the receiver operating characteristic curve (AUC). To have a better view of the whole procedure adopted by the solutions with the best results in terms of accuracy, since it is the metric adopted by all researchers, a more detailed description of the process applied by the authors of all articles found in this review whose prediction was higher than 95.00% is presented and summarized in Table 4.

Sampath and Baskar (2022) used 3D T1 weighted images acquired from 3 different databases: ADNI, OASIS, and AIBL, which at the processing level underwent resizing to improve the classification performance while using less memory, adaptive filtering to remove noise, adaptive histogram equalization for image enhancement and Voxel-based morphometry for segmentation of the ROI region, namely in terms of grey matter, white matter, and cerebrospinal fluid. In this solution, the authors applied several feature extraction methods after the pre-processing phase, namely grey-level co-occurrence matrices, which extract the numerical features using spatial correlations of similar grey levels, Gabor filtering to extract energy-based texture features, and Wavelet to extract the time-frequency representation. After that, a Hilbert-Schmidt independence criteria loop method was introduced to reduce more irrelevant features among those extracted from the MR images. Finally, the new investigation feature concerned the food source direction of the fish shoal optimizer (FSO) that was incorporated into the classification phase of the DSNN. The results obtained concerning Acc were very promising, with 99.89% for the ADNI database.

Raghavaiah and Varadarajan (2022) started from MR images and applied the following pre-processing techniques: skull removal, normalization, and GM, WM, and CSF segmentation using a clustering method that combines a temporally consistent black widow optimization (BWO) with a fuzzy C-means clustering (FCM). Regarding feature extraction, the authors implemented a hybrid TECD approach merged with clinical data to

TABLE 4 Summary of the best approaches found in this review.

A.	Dataset(s)	Image type	Data pre-processing	Data processing	Feature extraction + Segmentation	Classifier	ACC
Sampath and Baskar (2022)	ADNI AIBL OASIS	T1 sMRI	Resizing adaptive filtering for noise removal adaptive histogram equalization	Whole 3D image	GLCM Gabor filter wavelet features HSICL	FSODSNN based classifier	ADNI. CN vs. SMC vs. MCI vs. AD: 99.89% AIBL. CN vs. SMC vs. MCI vs. AD: 99.67% OASIS. CN vs. SMC vs. MCI vs. AD: 99.61%
Raghavaiah and Varadarajan (2022)	ADNI		Skull-stripping normalization TC-BWO-FCM for CSF, WM and GM segmentation	ROI-based	TECD feature extraction + Clinical features	HRF-DNN	AD vs. CN: 98.68% MCI vs. AD: 95.88% MCI vs. CN: 97.23%
Goenka and Tiwari (2022)	ADNI	T1 sMRI	N4 bias field correction skull stripping rigid registration	Whole 3D image		ConvNet	AD vs. CN: 97.83% AD vs. MCI: 98.68% CN vs. MCI: 99.10% CN vs. MCI vs. AD: 98.26%
Hazarika et al. (2021)	ADNI	T1 sMRI	Size scaling skull stripping	Slice-based		LeNet	AD vs. CN: 95.00% AD vs. MCI: 97.00% MCI vs. CN: 97.00%
Yan et al. (2022)	ADNI	T1 sMRI	Template registration skull-stripping filter denoising intensity normalization	Patch-based	SE mechanism PSA mechanism + FCN	MLP	AD vs. CN: 98.85%
Qasim Abbas et al. (2023)	ADNI	T1 sMRI	ACPC alignment correction intensity correction for uniform homogeneity skull-stripping registration	Whole 3D image	JD	CNN	AD vs. CN: 96.61%

add information concerning the patient's emotional condition. The TECD method characterizes the input image features based on statistical properties of image colours, grey level run length matrix, local discriminative powerful binary patterns, and tube density features by calculating each pixel's modified probability depending on its neighbours, and the clinical features including as to functional activities questionnaire, neuropsychiatric inventory and geriatric depression scale. This feature vector is given as input for the proposed deep rotation forest neural network to perform the classification task. Thus, the rotation forest creates the training data for the deep enhanced stacked autoencoder with a backpropagation learning classification algorithm. This HRF-DNN based solution obtained the following results in the binary classification tasks: AD vs. CN—98.68%, MCI vs. AD—95.88%, and MCI vs. CN—97.23%.

Goenka and Tiwari (2022) used 3D T1 sMRI images, on which the authors applied bias correction, skull-stripping, and rigid registration. Given the reduced size of the dataset, data augmentation techniques were used, namely: −5 and 5 degree angle rotations. Next, three ConvNets were created for three different input data processing approaches: hole 3D image, 3D patches, and slices. In the context of three-class categorization, a 14-layer architecture was employed with seven convolutional layers, four max-pooling layers, batch normalization, one global average pooling layer, and two dense layers. The same architecture with 14 layers was used in the 3D-Patch-based model, with a $72 \times 72 \times 72$ patch. The torch unfold function, which extracts sliding blocks from a batched input array, was employed to create these patches through a non-overlapping strategy. And finally, the 3D-Slice level ConvNet uses only 13 layers, with slight differences from as other two networks. The best results were achieved for the methodology applied to the whole image, with an accuracy of 99.10%

Hazarika et al. (2021) converted the 3D T1 weighted MR images into a group of 2D slices and identified the most suitable slices that can provide the regions of the hippocampus. Since the skull part is ignorable, skull-stripping and size scaling were applied. In this way, these images served as input for a LeNet network; however, instead of the traditional MaxPooling layer, the authors implemented a MinPooling layer in order also to evaluate the low-intensity pixels. This allowed the model to perform well, with an average accuracy of 96.64%.

Faisal and Kwon (2022) started by decreasing the size of the 3D T1 weighted MR images. The images were then divided into three slices: axial, coronal, and sagittal, with those at the beginning and end omitted as they contained no useful information. In addition, the slices were normalized with a mean and standard deviation of 0 (zero) and 1 (one), respectively. Consequently, the authors proposed a straightforward but powerful convolutional method (2D-CNN) that simultaneously carries out standard convolution, deep convolution, and point convolution, followed by a jumping convolution layer to learn multi-level characteristics from brain MRI data. The great feature of this model is the reduced amount of parameters and, consequently, the computational cost and speed of the model while achieving good results, namely 96.12% of classification accuracy between the CN, MCI, and AD classes.

Qasim Abbas et al. (2023) adopted four standard operations for pre-processing: ACPC alignment correction for identical orientation, skull removal to eliminate non-brain tissue, intensity correction for uniform homogeneity and image registration for geometric alignment in 3D T1 weighted sMRI. The Jacobian domain is then applied to the previously pre-processed images to create a Jacobian determinant map, which is then used to train a CNN model. The proposed architecture uses a sequential model consisting of one input, three convolutional, three max-pooling, one flattened, one fully connected, and one output layer(s). The effectiveness of the validation process determines the number of layers. The result obtained by this domain Jacobean convolutional neural network (JD-CNN), in terms of accuracy, was equal to 96.61% in the binary classification between CN and AD.

Yan et al. (2022) used MR-weighted 3D T1 weighted images, which in the processing underwent an affine transformation, skull removal, and filter denoising, including median filtering, Gaussian blur filtering, and anisotropic diffusion filtering, which was the one that showed the best results, and intensity normalization. After that, SE and PSA mechanisms were added to improve the used CNN's performance significantly. The SE mechanism obtains global data for each feature map by clustering the global average, and then a fully connected layer is implemented to identify the feature maps' global dependencies. At the same time, the PSA mechanism can manipulate spatial data of the input multi-scale feature maps and can successfully create long-term dependence among multi-scale channels' attention. Next, a FCN model was implemented, which consists of four convolutional blocks and two fully connected layers. A 3D convolutional layer, 3D maxpool layer, 3D batch normalization, Leaky ReLU, and Dropout are the convolutional block components. The final fully connected layers play a vital part in increasing the model's effectiveness, and the model is trained by random initialization of weights. The authors adopt a patch (of size equal to $47 \times 47 \times 47$) random sampling method from MRI scans to train the FCN model. In addition, the authors also construct the MLP model structure, which consists of two fully connected layers, batch normalization, Leaky ReLU, and Dropout. In the MLP model's image classification test, the authors pick the probability value of AD from disease probability map data, choose the ROI according to the MCC heat map of the FCN model, and match it with age, MMSE, and gender of the patients. The accuracy obtained by the used pipeline was 98.85% for the distinction between CN and AD.

5.1 | Reviews

Two systematic reviews were also taken into account in this review. Sethi et al. (2022) explored different AD classification methods based on CNNs. In this study, topics such as data pre-processing, data processing, 2D and 3D CNNs and their variants, and data augmentation and transfer learning, were addressed and compared. On the other hand, Tanveer et al. (2020) discussed machine learning techniques used in AD diagnosis,

TABLE 5 Summary of the reviews found in the current study.

A.	Years covered	Number of articles	Description
Sethi et al. (2022)	2012–2021	48	Analyse the efficacy of CNN classification approaches in AD using different datasets, neuroimaging modalities, and data pre-processing and processing techniques.
Tanveer et al. (2020)	2005–2019	165	The analysed machine learning methods are categorized into three main groups: support vector machine, artificial neural network, and deep learning and ensemble models.

namely support vector machine, artificial neural network, DL, and ensemble models. Within their study, they also evaluated different imaging modalities, feature extraction and selection techniques, and transfer learning. This information is summarized in Table 5.

6 | CONCLUSION

This literature review shows that the AD classification with neuroimaging is the subject of many studies based on different DL approaches. This review was focused on studies that at least used MRI data, which led to the exclusion of some studies obtained in the initial search. Nonetheless, other imaging techniques are less common in the clinical environment owing to the associated high costs.

As it was possible to perceive, several brain image datasets exist for studying Alzheimer's disease. Still, the ADNI dataset is the most used almost unanimously, providing a greater variety and quantity of samples.

It is undisputed that classification between AD and NC is the most straightforward task, leading to high accuracies, reaching almost 100% in some studies. However, it is not so clinically relevant as the predictions of sMCI to CN and pMCI to AD, which are more desirable but further challenging to reach good results. Regarding the implemented models, the results obtained in 2D or 3D approaches are similar, so it is impossible to conclude which is better. Both present limitations and advantages: 3D models represent more arduous challenges due to the increased number of parameters and computational cost, while in 2D approaches, not all information cannot be used as spatial relations are discarded.

Regarding the data approach adopted, most researchers opted for direct classification, with CNNs being the most predominant architecture. However, other methodologies that show potential to be explored, such as the RNN, are used in longitudinal data processing to extract the minimal differences between consecutive image scans on the same subject. When comparing this approach with feature extraction plus classification, it is difficult to draw many conclusions. However, it is possible to realize that it does not depend so much on the approach adopted but rather on the used models, parameters, and data processing. Time-to-event prognostic approaches are still little explored, with very few studies on the subject, but they have a promising future since they work in prediction.

Researchers widely use data augmentation and transfer learning techniques, which allow them to obtain promising performances even using small amounts of data.

Finally, by evaluating the best results presented in the reviewed articles, it was impossible to find a common characteristic to all, proving that several paths can be adopted in this area and still produce promising results.

In conclusion, this work essentially reviewed DL techniques to detect Alzheimer's disease in sMR images; however, as a possible future work, it would be interesting to extend this review by including other imaging modalities, such as fMRI or even PET.

AUTHOR CONTRIBUTIONS

Conceptualization and supervision by Martin Cerny and João Manuel R. S. Tavares; investigation, data collection, formal analysis, and original draft preparation by Mariana Coelho; writing review and editing by Martin Cerny and João Manuel R. S. Tavares.

CONFLICT OF INTEREST STATEMENT

The authors declare no conflict of interest.

DATA AVAILABILITY STATEMENT

Data sharing is not applicable to this article as no new data were created or analyzed in this study.

ORCID

Martin Cerny https://orcid.org/0000-0002-8893-2587
João Manuel R. S. Tavares https://orcid.org/0000-0001-7603-6526

REFERENCES

ADNI Alzheimer's disease neuroimaging initiative. https://adni.loni.usc.edu/

Agarwal, D., Berbis, M., Martín-Noguerol, T., Luna, A., Garcia, S., & Torre-Díez, L. I. (2022). End-to-end deep learning architectures using 3D neuroimaging biomarkers for early Alzheimer's diagnosis. *Mathematics*, *10*(15), 2575. https://doi.org/10.3390/math10152575

AIBL. https://aibl.csiro.au/

Al-Qerem, A., Salem, A. A., Jebreen, I., Nabot, A., & Samhan, A. (2021). Comparison between transfer learning and data augmentation on medical images classification. In *2021 22nd international Arab conference on information technology, ACIT 2021* (pp. 1–7). IEEE. https://doi.org/10.1109/ACIT53391.2021.9677144

Angkoso, C., Tjahyaningtijas, H., Purnomo, M., & Purnama, I. (2022). Multiplane convolutional neural network (Mp-CNN) for Alzheimer's disease classification. *International Journal of Intelligent Engineering and Systems*, *15*(1), 329–340. https://doi.org/10.22266/IJIES2022.0228.30

Asl, E. H., Ghazal, M., Mahmoud, A., Aslantas, A., Shalaby, A. M., Casanova, M. F., Barnes, G. N., Gimel'farb, G., Keynton, R., & El-Baz, A. (2018). Alzheimer's disease diagnostics by a 3D deeply supervised adaptable convolutional network. *Frontiers in Bioscience—Landmark*, *23*(3), 584–596. https://doi.org/10.2741/4606

Bae, J., Lee, S., Jung, W., Park, S., Kim, W., Oh, H., Han, J. W., Kim, G. E., Kim, J. S., Kim, J. H., & Kim, K. W. (2020). Identification of Alzheimer's disease using a convolutional neural network model based on T1-weighted magnetic resonance imaging. *Scientific Reports*, *10*(1), 22252. https://doi.org/10.1038/s41598-020-79243-9

Bae, J., Stocks, J., Heywood, A., Jung, Y., Jenkins, L., Hill, V., Katsaggelos, A., Popuri, K., Rosen, H., Beg, M. F., & Wang, L. (2021). Transfer learning for predicting conversion from mild cognitive impairment to dementia of Alzheimer's type based on a three-dimensional convolutional neural network. *Neurobiology of Aging*, *99*, 53–64. https://doi.org/10.1016/j.neurobiolaging.2020.12.005

Basaia, S., Agosta, F., Wagner, L., Canu, E., Magnani, G., Santangelo, R., & Filippi, M. (2019). Automated classification of Alzheimer's disease and mild cognitive impairment using a single MRI and deep neural networks. *NeuroImage: Clinical*, *21*, 101645. https://doi.org/10.1016/j.nicl.2018.101645

Basheera, S., & Ram, S. S. (2020). A novel CNN based Alzheimer's disease classification using hybrid enhanced ICA segmented gray matter of MRI. *Computerized Medical Imaging and Graphics*, *81*, 101713. https://doi.org/10.1016/j.compmedimag.2020.101713

Basher, A., Kim, B., Lee, K., & Jung, H. (2021). Volumetric feature-based Alzheimer's disease diagnosis from sMRI data using a convolutional neural network and a deep neural network. *IEEE Access*, *9*, 29870–29882. https://doi.org/10.1109/ACCESS.2021.3059658

Bi, X., Liu, W., Liu, H., & Shang, Q. (2021). Artificial intelligence-based MRI images for brain in prediction of Alzheimer's disease. *Journal of Healthcare Engineering*, *2021*, 8198552. https://doi.org/10.1155/2021/8198552

Cao, C., Liu, F., Tan, H., Song, D., Shu, W., Li, W., Zhou, Y., Bo, X., & Xie, Z. (2018). Deep learning and its applications in biomedicine. *Genomics, Proteomics & Bioinformatics*, *16*(1), 17–32. https://doi.org/10.1016/J.GPB.2017.07.003

Cobbinah, B., Sorg, C., Yang, Q., Ternblom, A., Zheng, C., Han, W., Che, L., & Shao, J. (2022). Reducing variations in multi-center Alzheimer's disease classification with convolutional adversarial autoencoder. *Medical Image Analysis*, *82*, 102585. https://doi.org/10.1016/j.media.2022.102585

Cui, R., & Liu, M. (2019a). Hippocampus analysis by combination of 3-D DenseNet and shapes for Alzheimer's disease diagnosis. *IEEE Journal of Biomedical and Health Informatics*, *23*(5), 2099–2107. https://doi.org/10.1109/JBHI.2018.2882392

Cui, R., & Liu, M. (2019b). RNN-based longitudinal analysis for diagnosis of Alzheimer's disease. *Computerized Medical Imaging and Graphics*, *73*, 1–10. https://doi.org/10.1016/j.compmedimag.2019.01.005

Despotović, I., Goossens, B., & Philips, W. (2015). MRI segmentation of the human brain: Challenges, methods, and applications. *Computational and Mathematical Methods in Medicine*, *2015*, 450341. https://doi.org/10.1155/2015/450341

Dyrba, M., Hanzig, M., Altenstein, S., Bader, S., Ballarini, T., Brosseron, F., Buerger, K., Cantré, D., Dechent, P., Dobisch, L., Düzel, E., Ewers, M., Fliessbach, K., Glanz, W., Haynes, J. D., Heneka, M. T., Janowitz, D., Keles, D. B., Kilimann, I., … Teipel, S. J. (2021). Improving 3D convolutional neural network comprehensibility via interactive visualization of relevance maps: Evaluation in Alzheimer's disease. *Alzheimer's Research and Therapy*, *13*(1), 191. https://doi.org/10.1186/s13195-021-00924-2

Faisal, F., & Kwon, G. R. (2022). Automated detection of Alzheimer-s disease and mild cognitive impairment using whole brain MRI. *IEEE Access*, *10*, 65055–65066. https://doi.org/10.1109/ACCESS.2022.3180073

Fan, Z., Li, J., Zhang, L., Zhu, G., Li, P., Lu, X., Shen, P., Shah, S. A. A., Bennamoun, M., Hua, T., & Wei, W. (2021). U-net based analysis of MRI for Alzheimer's disease diagnosis. *Neural Computing and Applications*, *33*(20), 13587–13599. https://doi.org/10.1007/s00521-021-05983-y

Folego, G., Weiler, M., Casseb, R., Pires, R., & Rocha, A. (2020). Alzheimer's disease detection through whole-brain 3D-CNN MRI. *Frontiers in Bioengineering and Biotechnology*, *8*, 534592. https://doi.org/10.3389/fbioe.2020.534592

Goenka, N., & Tiwari, S. (2022). AlzVNet: A volumetric convolutional neural network for multiclass classification of Alzheimer's disease through multiple neuroimaging computational approaches. *Biomedical Signal Processing and Control*, *74*, 103500. https://doi.org/10.1016/j.bspc.2022.103500

Goyal, P., Rani, R., & Singh, K. (2022). State-of-the-art machine learning techniques for diagnosis of Alzheimer's disease from MR-images: A systematic review. *Archives of Computational Methods in Engineering*, *29*(5), 2737–2780. https://doi.org/10.1007/s11831-021-09674-8

Guan, H., Wang, C., Cheng, J., Jing, J., & Liu, T. (2022). A parallel attention-augmented bilinear network for early magnetic resonance imaging-based diagnosis of Alzheimer's disease. *Human Brain Mapping*, *43*(2), 760–772. https://doi.org/10.1002/hbm.25685

Hazarika, R., Abraham, A., Kandar, D., & Maji, A. (2021). An improved LeNet-deep neural network model for Alzheimer's disease classification using brain magnetic resonance images. *IEEE Access*, *9*, 161194–161207. https://doi.org/10.1109/ACCESS.2021.3131741

Huang, Y., Xu, J., Zhou, Y., Tong, T., & Zhuang, X. (2019). Diagnosis of Alzheimer's disease via multi-modality 3D convolutional neural network. *Frontiers in Neuroscience*, *13*(MAY), 509. https://doi.org/10.3389/fnins.2019.00509

Jiang, J., Zhang, J., Li, Z., Li, L., & Huang, B. (2022). Using deep learning Radiomics to distinguish cognitively Normal adults at risk of Alzheimer's disease from Normal control: An exploratory study based on structural MRI. *Frontiers in Medicine*, *9*, 894726. https://doi.org/10.3389/fmed.2022.894726

Khagi, B., Lee, K., Choi, K., Lee, J., Kwon, G. R., & Yang, H. D. (2021). VBM-based Alzheimer's disease detection from the region of interest of T1 MRI with supportive Gaussian smoothing and a Bayesian regularized neural network. *Applied Sciences (Switzerland)*, *11*(13), 6175. https://doi.org/10.3390/app11136175

Lee, G., Nho, K., Kang, B., Sohn, K. A., Kim, D., for Alzheimer's Disease Neuroimaging Initiative, Weiner, M. W., Aisen, P., Petersen, R., Jack, C. R., Jr., Jagust, W., Trojanowki, J. Q., Toga, A. W., Beckett, L., Green, R. C., Saykin, A. J., Morris, J., Shaw, L. M., Khachaturian, Z., … Fargher, K. (2019). Predicting

Alzheimer's disease progression using multi-modal deep learning approach. *Scientific Reports*, *9*(1), 1–12. https://doi.org/10.1038/s41598-018-37769-z

Li, C., Wang, Q., Liu, X., & Hu, B. (2022). An attention-based CoT-ResNet with channel shuffle mechanism for classification of Alzheimer's disease levels. *Frontiers in Aging Neuroscience*, *14*, 930584. https://doi.org/10.3389/fnagi.2022.930584

Li, F., & Liu, M. (2018). Alzheimer's disease diagnosis based on multiple cluster dense convolutional networks. *Computerized Medical Imaging and Graphics*, *70*, 101–110. https://doi.org/10.1016/j.compmedimag.2018.09.009

Li, F., & Liu, M. (2019). A hybrid convolutional and recurrent neural network for hippocampus analysis in Alzheimer's disease. *Journal of Neuroscience Methods*, *323*, 108–118. https://doi.org/10.1016/j.jneumeth.2019.05.006

Li, J., Wei, Y., Wang, C., Hu, Q., Liu, Y., & Xu, L. (2022). 3-D CNN-based multichannel contrastive learning for Alzheimer's disease automatic diagnosis. *IEEE Transactions on Instrumentation and Measurement*, *71*, 1–11. https://doi.org/10.1109/TIM.2022.3162265

Liang, X., Wang, Z., Chen, Z., & Song, X. (2022). Alzheimer's disease classification using distilled multi-residual network. *Applied Intelligence*, *53*, 11934–11950. https://doi.org/10.1007/s10489-022-04084-0

Lim, B., Lai, K., Haiskin, K., Kulathilake, K. A. S. H., Ong, Z. C., Hum, Y. C., Dhanalakshmi, S., Wu, X., & Zuo, X. (2022). Deep learning model for prediction of progressive mild cognitive impairment to Alzheimer's disease using structural MRI. *Frontiers in Aging Neuroscience*, *14*, 876202. https://doi.org/10.3389/fnagi.2022.876202

Liu, C. F., Padhy, S., Ramachandran, S., Wang, V. X., Efimov, A., Bernal, A., Shi, L., Vaillant, M., Ratnanather, J. T., Faria, A. V., Caffo, B., Albert, M., Miller, M. I., BIOCARD Research Team, & Alzheimer's Disease Neuroimaging Initiative. (2019). Using deep Siamese neural networks for detection of brain asymmetries associated with Alzheimer's disease and mild cognitive impairment. *Magnetic Resonance Imaging*, *64*, 190–199. https://doi.org/10.1016/j.mri.2019.07.003

Liu, M., Li, F., Yan, H., Wang, K., Ma, Y., Alzheimer's Disease Neuroimaging Initiative, Shen, L., & Xu, M. (2020). A multi-model deep convolutional neural network for automatic hippocampus segmentation and classification in Alzheimer's disease. *NeuroImage*, *208*, 116459. https://doi.org/10.1016/j.neuroimage.2019.116459

Liu, Z., Lu, H., Pan, X., Xu, M., Lan, R., & Luo, X. (2022). Diagnosis of Alzheimer's disease via an attention-based multi-scale convolutional neural network. *Knowledge-Based Systems*, *238*, 107942. https://doi.org/10.1016/j.knosys.2021.107942

Mansour, L. S., Seguin, C., Smith, R. E., & Zalesky, A. (2022). Connectome spatial smoothing (CSS): Concepts, methods, and evaluation. *NeuroImage*, *250*, 118930. https://doi.org/10.1016/J.NEUROIMAGE.2022.118930

Mendoza-Léon, R., Puentes, J., Uriza, L., & Hernández, H. M. (2020). Single-slice Alzheimer's disease classification and disease regional analysis with supervised switching autoencoders. *Computers in Biology and Medicine*, *116*, 103527. https://doi.org/10.1016/j.compbiomed.2019.103527

Nanni, L., Interlenghi, M., Brahnam, S., Salvatore, C., Papa, S., Nemni, R., Castiglioni, I., & Alzheimer's Disease Neuroimaging Initiative. (2020). Comparison of transfer learning and conventional machine learning applied to structural brain MRI for the early diagnosis and prognosis of Alzheimer's disease. *Frontiers in Neurology*, *11*, 576194. https://doi.org/10.3389/fneur.2020.576194

OASIS Brains: Open access series of imaging studies. https://www.oasis-brains.org/

Ocasio, E., & Duong, T. (2021). Deep learning prediction of mild cognitive impairment conversion to Alzheimer's disease at 3 years after diagnosis using longitudinal and wholebrain 3D MRI. *PeerJ Computer Science*, *7*, 1–21. https://doi.org/10.7717/PEERJ-CS.560

Odusami, M., Maskeliūnas, R., & Damaševičius, R. (2022). An intelligent system for early recognition of Alzheimer's disease using neuroimaging. *Sensors*, *22*(3), 740. https://doi.org/10.3390/s22030740

Qasim Abbas, S., Chi, L., & Chen, Y. P. (2023). Transformed domain convolutional neural network for Alzheimer's disease diagnosis using structural MRI. *Pattern Recognition*, *133*, 109031. https://doi.org/10.1016/j.patcog.2022.109031

Raghavaiah, P., & Varadarajan, S. (2021). A CAD system design to diagnosize Alzheimers disease from MRI brain images using optimal deep neural network. *Multimedia Tools and Applications*, *80*(17), 26411–26428. https://doi.org/10.1007/s11042-021-10928-7

Raghavaiah, P., & Varadarajan, S. (2022). A CAD system design for Alzheimer's disease diagnosis using temporally consistent clustering and hybrid deep learning models. *Biomedical Signal Processing and Control*, *75*, 103571. https://doi.org/10.1016/j.bspc.2022.103571

Razzak, I., Naz, S., Ashraf, A., Khalifa, F., Bouadjenek, M., & Mumtaz, S. (2022). Mutliresolutional ensemble PartialNet for Alzheimer detection using magnetic resonance imaging data. *International Journal of Intelligent Systems*, *37*(10), 6613–6630. https://doi.org/10.1002/int.22856

Razzak, M. I., Naz, S., & Zaib, A. (2018). Deep learning for medical image processing: Overview, challenges and the future. In N. Dey, A. Ashour, & S. Borra (Eds.), *Classification in BioApps: Automation of decision making* (Vol. 26, pp. 323–350). Springer.

Reiman, E. M., & Jagust, W. J. (2012). Brain imaging in the study of Alzheimer's disease. *NeuroImage*, *61*(2), 505–516. https://doi.org/10.1016/J.NEUROIMAGE.2011.11.075

Sampath, R., & Baskar, M. (2022). 3D brain image-based Alzheimer's disease detection techniques using fish swarm optimizer's deep convolution Siamese neural network. *Expert Systems*, *39*(9), e12963. https://doi.org/10.1111/exsy.12963

Saratxaga, C. L., Moya, I., Picón, A., Acosta, M., Moreno-Fernandez-de-Leceta, A., Garrote, E., & Bereciartua-Perez, A. (2021). MRI deep learning-based solution for Alzheimer's disease prediction. *Journal of Personalized Medicine*, *11*(9), 902. https://doi.org/10.3390/jpm11090902

Sethi, M., Ahuja, S., Rani, S., Koundal, D., Zaguia, A., & Enbeyle, W. (2022). An exploration: Alzheimer's disease classification based on convolutional neural network. *BioMed Research International*, *2022*, 8739960. https://doi.org/10.1155/2022/8739960

Shaji, S., Ganapathy, N., & Swaminathan, R. (2021). Classification of Alzheimer condition using MR brain images and inception-residual network model. *Current Directions in Biomedical Engineering*, *7*(2), 763–766. https://doi.org/10.1515/cdbme-2021-2195

Sharma, R., Goel, T., Tanveer, M., Lin, C., Fellow, I., & Raman, M. (2023). Deep learning based diagnosis and prognosis of Alzheimer's disease: A comprehensive review. *IEEE Transactions on Cognitive and Developmental Systems*, *15*, 1123–1138. https://doi.org/10.1109/TCDS.2023.3254209

Shukla, A., Tiwari, R., & Tiwari, S. (2023). Review on Alzheimer disease detection methods: Automatic pipelines and machine learning techniques. *Sci*, *5*(1), 13. https://doi.org/10.3390/sci5010013

Suh, C. H., Shim, W. H., Kim, S. J., Roh, J. H., Lee, J. H., Kim, M. J., Park, S., Jung, W., Sung, J., Jahng, G. H., & for the Alzheimer's Disease Neuroimaging Initiative. (2020). Development and validation of a deep learning-based automatic brain segmentation and classification algorithm for Alzheimer disease using 3D T1-weighted volumetric images. *American Journal of Neuroradiology*, *41*(12), 2227–2234. https://doi.org/10.3174/ajnr.A6848

Tanveer, M., Richhariya, B., Khan, R. U., Rashid, A. H., Khanna, P., Prasad, M., & Lin, C. T. (2020). Machine learning techniques for the diagnosis of Alzheimer's disease: A review. *ACM Transactions on Multimedia Computing, Communications and Applications*, *16*(1s), 1–35. https://doi.org/10.1145/3344998

Vadmal, V., Junno, G., Badve, C., Huang, W., Waite, K. A., & Barnholtz-Sloan, J. S. (2020). MRI image analysis methods and applications: An algorithmic perspective using brain tumors as an exemplar. *Neuro-Oncology Advances*, *2*(1), 1–13. https://doi.org/10.1093/NOAJNL/VDAA049

Wang, C., Li, Y., Tsuboshita, Y., Sakurai, T., Goto, T., Yamaguchi, H., Yamashita, Y., Sekiguchi, A., Tachimori, H., for the Alzheimer's Disease Neuroimaging Initiative, Wang, C., Li, Y., & Goto, T. (2022). A high-generalizability machine learning framework for predicting the progression of Alzheimer's disease using limited data. *Npj Digital Medicine*, *5*(1), 43. https://doi.org/10.1038/s41746-022-00577-x

Wen, J., Thibeau-Sutre, E., Diaz-Melo, M., Samper-González, J., Routier, A., Bottani, S., Dormont, D., Durrleman, S., Burgos, N., Colliot, O., Alzheimer's Disease Neuroimaging Initiative, & Australian Imaging Biomarkers and Lifestyle flagship study of ageing. (2020). Convolutional neural networks for classification of Alzheimer's disease: Overview and reproducible evaluation. *Medical Image Analysis*, *63*, 101694. https://doi.org/10.1016/j.media.2020.101694

Yan, B., Li, Y., Li, L., Yang, X., Li, T. Q., Yang, G., & Jiang, M. (2022). Quantifying the impact of pyramid squeeze attention mechanism and filtering approaches on Alzheimer's disease classification. *Computers in Biology and Medicine*, *148*, 105944. https://doi.org/10.1016/j.compbiomed.2022.105944

Yiğit, A., & Işik, Z. (2020). Applying deep learning models to structural MRI for stage prediction of Alzheimer's disease. *Turkish Journal of Electrical Engineering and Computer Sciences*, *28*(1), 196–210. https://doi.org/10.3906/elk-1904-172

Zhang, F., Li, Z., Zhang, B., Du, H., Wang, B., & Zhang, X. (2019). Multi-modal deep learning model for auxiliary diagnosis of Alzheimer's disease. *Neurocomputing*, *361*, 185–195. https://doi.org/10.1016/j.neucom.2019.04.093

Zhao, Y., Ma, B., Jiang, P., Zeng, D., Wang, X., & Li, S. (2021). Prediction of Alzheimer's disease progression with multi-information generative adversarial network. *IEEE Journal of Biomedical and Health Informatics*, *25*(3), 711–719. https://doi.org/10.1109/JBHI.2020.3006925

AUTHOR BIOGRAPHIES

Mariana Coelho received the Graduate degree in biomedical engineering from the Instituto Superior de Engenharia do Porto (ISEP), Porto, Portugal in 2020, and the M.Sc. degree in biomedical engineering from the Faculdade de Engenharia da Universidade do Porto (FEUP), Porto, Portugal in 2023. Her main research interests include computational vision, medical imaging, artificial intelligence, and data science and analysis.

Martin Cerny received the M.Sc. degree in the specialization measurement and control in biomedical engineering and the Ph.D. degree in technical cybernetics with focus on biomedical engineering from the Faculty of Electrical Engineering and Computer Science, VSB-Technical University of Ostrava (TUO), Ostrava, Czech Republic, in 2005 and 2012, respectively. He worked as a Post-Ph.D. Researcher at the VSB-TUO with stay at Institute for Nanotechnology of Lyon, Villeurbanne, France. He is currently an Associate Professor at the Department of Cybernetic and Biomedical Engineering, VSB–TUO. He is specialized in biomedical engineering, telemedicine, inertial sensors, and remote home care systems. He is responsible of Living Laboratory at VSB - Technical university of Ostrava focused on modern technologies for elderly and disabled persons, study branch focused on biomedical assistive technologies.

João Manuel R. S. Tavares graduated in Mechanical Engineering at the Universidade do Porto, Portugal in 1992. He also earned his M.Sc. degree and Ph.D. degree in Electrical and Computer Engineering from the Universidade do Porto in 1995 and 2001, and attained his Habilitation in Mechanical Engineering in 2015 from the same University. He is a senior researcher at the Instituto de Ciência e Inovação em Engenharia Mecânica e Engenharia Industrial (INEGI) and Full Professor at the Department of Mechanical Engineering (DEMec) of the Faculdade de Engenharia da Universidade do Porto (FEUP). He has been the Head of DEMec since June 2023. João Tavares is co-editor of more than 80 books, co-author of more than 50 book chapters, 650 articles in international and national journals and conferences, and 3 international and 3 national patents. He has been a committee member of several international and national journals and conferences, is co-founder and co-editor of the book series “Lecture Notes in Computational Vision and Biomechanics” published by Springer, founder and Editor-in-Chief of the journal “Computer Methods in Biomechanics and Biomedical Engineering: Imaging & Visualization” published by Taylor & Francis, Editor-in-Chief of the journal “Computer Methods in Biomechanics and Biomedical Engineering” published by Taylor & Francis, and co-founder and co-chair of the international conference series: International Symposium on Computational Modeling of Objects Presented in Images, ECCOMAS Thematic Conference on Computational Vision and Medical Image Processing, International Conference on Computational and Experimental Biomedical Sciences and International Conference on Biodental Engineering. Additionally, he has been (co-)supervisor of several MSc and PhD thesis and supervisor of several post-doc projects, and has participated in many scientific projects both as researcher and as scientific coordinator. His main research areas include computational vision, medical imaging, scientific visualization, biomechanics, biomedical engineering, and new product development.

How to cite this article: Coelho, M., Cerny, M., & Tavares, J. M. R. S. (2025). Deep learning methods to detect Alzheimer's disease from MRI: A systematic review. *Expert Systems*, *42*(1), e13463. https://doi.org/10.1111/exsy.13463